



## A NONLINEAR DYNAMIC MODEL FOR COLLAPSE INVESTIGATIONS IN TALL TIMBER BUILDINGS – PRELIMINARY RESULTS

Alex Sixie Cao<sup>1</sup>, Lukas Esser<sup>2</sup>, Ben Glarner<sup>3</sup> Andrea Frangi<sup>4</sup>

**ABSTRACT:** Structural robustness of timber buildings is becoming increasingly relevant because of the increasing use of timber in the built environment. An important tool for assessing the robustness of any structure is an efficient numerical model capable of simulating progressive collapse. With such a model, physical tests can be limited to a few carefully selected validation tests and the robustness of a wide range of building typologies and geometries can be investigated efficiently. In this paper, a parametric nonlinear dynamic model for simulating progressive collapse of timber buildings is presented. Because of the parametric capabilities of the model, a vast range of buildings can be modelled. Moreover, the entirety of a collapse can be simulated with the recently developed mixed element method and the implementation of stress- and energy-based failure criteria for normal loading and impact loading. To demonstrate the capabilities of the model, a case study is presented on a symmetrical three-dimensional frame building with varying cross-sectional member dimensions. The model is an indispensable tool for investigating the robustness of timber buildings.

**KEYWORDS:** Structural robustness, Progressive collapse, Nonlinear dynamic modelling, Impact loading, OpenSees

### 1 INTRODUCTION

Buildings and other infrastructure are essential in our daily life. They provide us with shelter from the weather, working and leisure spaces, and they serve logistical purposes in our society. When a building is damaged, it may lose its main function of providing shelter and instead become a hazard to its users. To limit such hazards, buildings should be built such that the damage can be confined, and a disproportionate and progressive collapse can be prevented. This property of a structure is its structural robustness, which can be defined as the insensitivity to initial damage [1].

After the progressive collapses of Ronan Point in 1968 and the World Trade Center in 2001 [2,3], substantial efforts have been put into research on the robustness of steel and reinforced concrete structures [3]. At present, most of the building stock in Europe comprises reinforced concrete and masonry buildings [4]. As the use of timber in our built environment is being increasingly recognized as an important carbon sequestration tool [5], more and more timber buildings are also being built [6–8]. However, the knowledge on structural robustness of timber buildings is still scarce [3,9,10].

Dissimilar to steel and reinforced concrete, timber is an intrinsically lightweight material [11,12]. This leads to vastly different behaviour when subjected to lateral loading, such as wind and seismic loading [12–15]. Besides the weight difference, the material and its connections are also dissimilar to its conventional steel and reinforced concrete opponents [16–18]. Therefore, existing knowledge on the robustness of steel and

reinforced concrete structures cannot be directly applied to timber buildings [10].

To assess the robustness of any structure, one of the primary tools is an efficient and accurate numerical model [3]. Because of the complexity of the behaviour of timber and its connections, and the highly dynamic nature of a collapse, a nonlinear dynamic model accounting for large deformations is necessary [3,9,19]. [3,9] With such a model, the structural robustness of a vast range of buildings and materials can be investigated, and physical experiments can be reduced to a few validation tests of the model.

In this paper, a fully parametric nonlinear dynamic model for simulating progressive collapse of timber buildings is presented. The model can simulate the entirety of a progressive collapse with large deformations and incremental damping. To facilitate the separation, detachment, and loss of members, the recently developed mixed element method was implemented [20]. Besides commonly used stress-based failure criteria [21], an energy-based failure criterion based on extensive impact tests on full-size timber beams was used [22–25]. The collapse model was written in Python with the open-source finite element framework OpenSees [26].

To demonstrate the model, a three-dimensional frame subjected to a corner, edge, and internal ground-floor column removal was analysed. The frame comprises glued laminated timber beams and columns, and laterally loaded dowel-type connections with slotted-in steel plates. The frames are designed for the vertical gravity loads in the ultimate and serviceability limit states, as well as serviceability-level wind-induced vibrations.

<sup>1</sup> Alex Sixie Cao, Institute of Structural Engineering, ETH Zurich, 8093 Zurich, Switzerland, [cao@ibk.baug.ethz.ch](mailto:cao@ibk.baug.ethz.ch)

<sup>2</sup> Lukas Esser, Institute of Structural Engineering, ETH Zurich, 8093 Zurich, Switzerland, [lukas.esser@ibk.baug.ethz.ch](mailto:lukas.esser@ibk.baug.ethz.ch)

<sup>3</sup> Ben Glarner, Institute of Structural Engineering, ETH Zurich, 8093 Zurich, Switzerland

<sup>4</sup> Andrea Frangi, Institute of Structural Engineering, ETH Zurich, 8093 Zurich, Switzerland, [frangi@ibk.baug.ethz.ch](mailto:frangi@ibk.baug.ethz.ch)

## 2 MODEL DESCRIPTION

### 2.1 CONCEPTUAL FRAMEWORK

The conceptual framework comprises the seven different modules shown in Figure 1. In the framework's development, a basic requirement was the ability to have a fully parametric model with a programmable input interface of the different model parameters. To accommodate this requirement, the building geometry was constrained to an irregular orthogonal grid. This enables an irregular positioning of the orthogonal grid axes, which makes different bay lengths and floor heights possible. Beam elements can be positioned on any of the grid axes, and shell elements can be positioned on any of the three surface planes following the grid. In the future, trusses will be implemented following the same system. For the programmable input interface, a matrix equivalent representation of the building was developed. These features are shown in Figure 1a.

Another requirement was the possibility of adapting the model to commonly used connections in timber buildings, such as laterally loaded dowel-type connections and axially loaded dowel-type connections. It is also possible to implement connection models with hysteresis. The parametric connection model is shown in Figure 1b.

It was decided that the framework would be required to simulate the entirety of a collapse. For this purpose, the mixed element method was developed and verified [20]. The method uses finite elements with physical lengths and properties, interspersed with rigid zero-length elements. For each time-step, a failure detection algorithm detects the exceedance of a failure criterion in the model and removes the rigid zero-length elements at the points of failure. With this, the simulation can continue after the failure of a building member. This is shown in Figure 1c. To impose initial damage scenarios and to remove elements in the analysis upon failure, an element removal

algorithm was developed [27]. The real removal of these elements is advantageous over a stiffness reduction approach, since the stiffness reduction approach may lead to convergence problems. The element removal algorithm is shown in Figure 1d.

If a rigid zero-length element is removed such that a finite element with physical length is entirely disconnected from the rest of the model, a convergence problem would occur. To avoid such convergence problems, any disconnected parts of the model with rigid-body motions were removed. The removal was conducted with the element removal algorithm shown in Figure 1d. In reality, the rigid-body motion of the removed parts would be building debris, which would lead to impact loading at some point. Therefore, a debris tracking algorithm was implemented for any parts with rigid-body motion. The debris tracking algorithm calculates the trajectory of the debris as projectiles. This is shown in Figure 1e.

Besides the debris tracking algorithm, an impact detection and loading algorithm was developed. If the impact detection algorithm detects debris is impacting a member of the remaining structure, the impact loading algorithm is activated. This loads the impacted member over a pre-determined time-step and is shown in Figure 1f.

Based on impact tests of full-size glued laminated timber beams [22–25], an energy-based failure criterion was developed, and the impact time was found. If the kinetic energy of the debris exceeds the energy capacity given by the failure criterion, local failure of the member will occur. This is shown in Figure 1g.

### 2.2 ANALYSIS DESCRIPTION

The conceptual framework of the collapse model in Section 2.1 was implemented in Python, with the open-source finite element framework OpenSeesPy [26] as the computational engine. To organise the input and output of

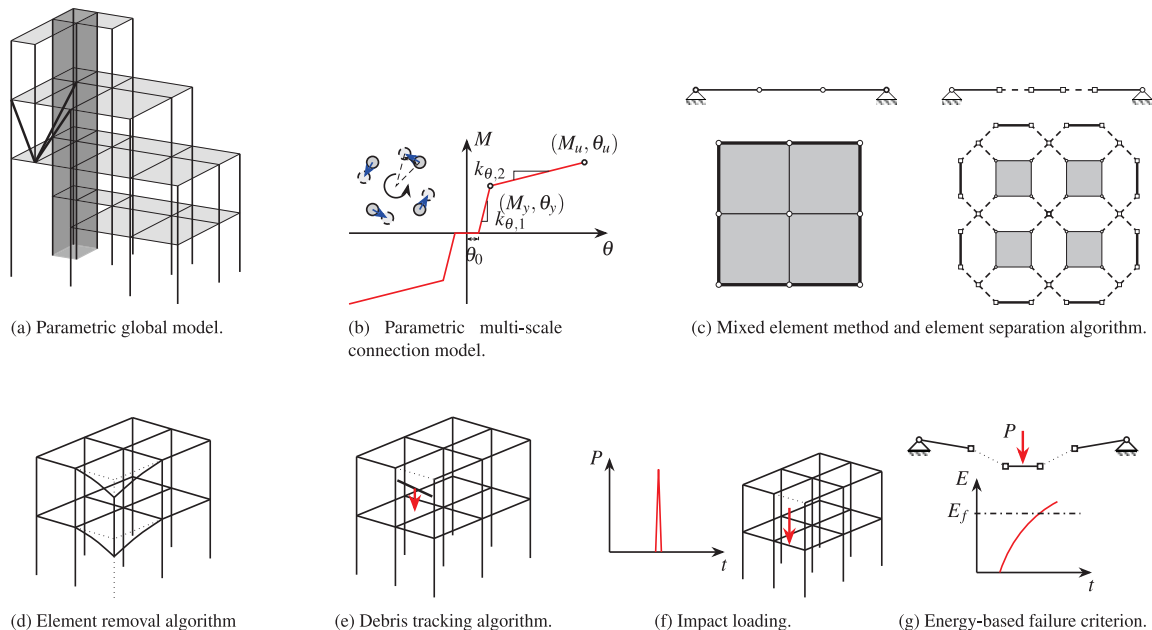


**Figure 1:** Conceptual framework of the collapse model and figurative illustrations of the different modules.

the model, an SQL database was developed with SQLite in Python. In the general framework, one-dimensional *forceBeamColumn* elements were implemented for the beams and the columns, and two-dimensional *ShellMITC4* elements were implemented for wall and slab members. The connections and the rigid links interspersed between the finite elements were modelled with the zero-length element *twoNodeLink*. The beam and column members were modelled with a linear-elastic perfectly brittle material behaviour, which is concurrent with high strain-rate models for glued laminated timber [28]. As a simplification, the connections were also modelled as a linear-elastic perfectly brittle material. A corotational transformation was used for the entire model.

### 2.2.1 Element-removal algorithm

The element-removal algorithm can be described in the following steps:

1. Solve the system of equations to get the internal forces of the element to be removed.
2. Remove the element from the model and re-apply the internal forces of the removed element.
3. Step down the internal forces of the removed element linearly over a time  $t_r$ .

The algorithm can be used for static or dynamic analysis and can also be used for the removal of entire members. In the collapse model, it is used for in situ removal of any failed elements, detached model parts with rigid-body motion, and to impose damage by removing single elements or members. A full description of the element removal algorithm can be found in Cao et al. [27].

For a column-removal scenario, the UFC 4-023-03 [29] states that the removal time  $t_r$  must be less than  $1/10$  of the natural period of the vibration mode associated with the damage, whereas ASCE 7-22 recommends an impact duration between 30 ms for modelling flood-borne debris. In EN 1991-1-7 [30], hard impact for vehicles results an impact time of 70 ms. The results from the impact tests conducted by Cao et al. [22–25] showed that the mean impact time was 12 ms, with an impact velocity of around 9.6 m/s, which corresponds to a free-fall of about 4.7 m. The natural period associated with the initial damage scenario was in the order of 400 ms. On this basis, a removal time  $t_r$  of 20 ms was chosen.

### 2.2.2 Incremental damping

One of the main drawbacks of previous models was the lack of an incremental damping formulation [31], which is also a general weakness for the most common damping implementations [32]. During a collapse, the connections and members may enter the nonlinear range and parts of the building may detach from the surviving structure. Because of the potential nonlinearities of the members, the stiffness of the system may change. Similarly, the detached parts do not contribute to the mass or stiffness of the remaining building. Therefore, a damping scheme which does not account for the changes in the stiffness and mass of the building during a collapse may lead to gross errors. Moreover, modal analysis in the undamaged state will not reflect the vibration modes throughout a collapse.

In the current state of the model, an incremental damping scheme based on Rayleigh damping is implemented. Rayleigh damping considers both stiffness- and mass-proportionate damping in the damping matrix  $\mathbf{C}$ :

$$\mathbf{C} = \alpha \mathbf{M} + \beta \mathbf{K}, \quad (1)$$

where  $\mathbf{M}$  is the mass matrix,  $\mathbf{K}$  is the stiffness matrix, and  $\alpha$  and  $\beta$  are calibration parameters. The calibration parameters  $\alpha$  and  $\beta$  are selected based on the natural angular frequency  $\omega_i$  and  $\omega_j$  of two vibration modes or frequencies from an eigenvalue analysis, which determine the range of interest for the damping scheme. The two calibration parameters  $\alpha$  and  $\beta$  can be computed from:

$$\alpha = \zeta \frac{2\omega_i\omega_j}{\omega_i + \omega_j}, \quad \beta = \zeta \frac{2}{\omega_i + \omega_j}, \quad (2)$$

where  $\zeta$  is the damping ratio. Because the vibration modes at the undamaged state of the model will not reflect the vibration modes throughout the collapse, the iterative damping scheme is based on updating the mass  $\mathbf{M}$  and stiffness  $\mathbf{K}$  matrices at each time-step. By doing so, nonlinearities and physical detachments of building parts will be reflected in the damping  $\mathbf{C}$  of the analysis. The calibration parameters  $\alpha$  and  $\beta$  are only computed at the start of the analysis because of difficulties with high-frequency modes  $\omega_i$  and instabilities throughout the simulation. To avoid the calibration parameters  $\alpha$  and  $\beta$  coefficients from being computed too close to each other, the frequency  $j$  was set as  $\omega_j = 5\omega_i$ , and frequency  $i$  was set as the first natural frequency  $\omega_i = \omega_1$ .

### 2.2.3 Convergence check

The dynamic analysis was conducted with an implicit time integration scheme. For the implicit integration, the unconditionally stable average acceleration method in the Newmark family is used. To solve the nonlinear equations of motion, the Newton-Raphson method was used.

Because the failure criteria in the model are checked at each time-step, an optimum maximum time-step had to be determined. If the maximum time-step is too large, the utilization of the members will grossly exceed the capacity. If the maximum time-step is too small, the model will be computationally inefficient. Based on a sensitivity analysis of the maximum time-step, a time-step of 0.5 ms was used for the collapse simulations. Compared to a time-step of 0.1 ms, the difference in the time of the last element failure was about 1.6%. The difference in the vertical deflections of the node above the removed column was about 4.6%, and the maximum utilization in the model was 1.08, compared to 1.04 for a time-step of 0.1 ms.

Like the sensitivity analysis of the maximum time-step, a mesh sensitivity analysis was conducted to determine the best member discretization. A member discretization of five finite elements per member was found as the optimum between computational expenses and accuracy. Compared with a discretization of ten finite elements per member, the difference in the time of the last element failure was about 0.2%, and the difference in the vertical deflections of the node above the removed column was about 0.8%. The computation time of the simulation was approximately 56% shorter for the discretization with five

finite elements per member. The incremental Rayleigh damping scheme in Section 2.2.2 was calibrated for the first and fifth vibration modes.

### 2.3 FAILURE CRITERIA

For most of the failure checks in the model, stress-based failure criteria according to EN 1995-1-1:2004 [21] were used at each time-step. The design checks were conducted on the mean material strength level, without load factors on the action side. The connections were modelled as linear elastic and perfectly brittle in rotation, with a maximum allowable rotation  $\theta_y$  of 25.8 mrad, or a moment  $M_y$  of 52.4 kNm. For the mean material strengths, parameters from Schilling et al. [33] were used for glued laminated timber of strength class GL24h. For the mean elastic and shear modulus, values from EN 14080:2013 [34] were used for GL24h.

#### 2.3.1 Combined compression and bending action

In the model, a corotational transformation was used. The corotational transformation is suitable for problems with large deformations, which are expected during a collapse. Because of the corotational transformation, a second order failure criterion for combined compression and bending action can be used without buckling coefficients. This is possible because second order P- $\Delta$ -effects are automatically considered in the equilibrium computations. Therefore, the failure criterion for combined compression and bending action was:

$$\frac{\sigma_{c,0}}{f_{c,0}} + \frac{\sigma_{m,y} + \sigma_{m,z}}{f_m} \leq 1, \quad (3)$$

where  $\sigma_{c,0}$  is the compressive stress parallel to the grain,  $f_{c,0}$  is the compressive strength parallel to the grain,  $\sigma_{m,y}$  and  $\sigma_{m,z}$  are the maximum bending stresses about the strong and weak axis of the cross-section, and  $f_m$  is the bending strength.

#### 2.3.2 Energy-based failure criterion

In this paper, the energy-based failure criterion was based on work done on impact loading of timber beams at ETH Zurich [22–25]. Because of the dynamic nature of impact loading, a limit state based on energy was used instead of one based on stresses. From the pendulum impact hammer tests on full-size timber beams, the failure energy  $E_r$  was determined directly. The failure energy  $E_r$  from the tests is analogous to the strength of a material in terms of stresses. If the strain energy in the member  $E_s$  from imposed loads exceeds the failure energy  $E_r$ , the member has failed. This can be expressed as:

$$E_s \leq E_r \Leftrightarrow \frac{E_s}{E_r} \leq 1. \quad (4)$$

If the kinetic energy of a projectile from impact loading  $E_k$  is considered as well, Equation (4) can be expanded to:

$$\frac{E_s + E_k}{E_r} \leq 1. \quad (5)$$

The kinetic energy of a projectile can be computed from  $E_k=0.5mv^2$ , where  $m$  is the mass of the projectile, and  $v$  is the velocity of the projectile. The velocity  $v$  of the

projectile can be found directly from classical projectile motion, with the initial velocity vector  $\mathbf{v}$  from the collapse model. From the impact tests, the failure energy  $E_r$  of the beams in this paper is 22.2 kJ.

## 3 FRAME DESIGN AND SIMULATIONS

### 3.1 DESIGN OF FRAMES

The design of the frames was conducted for gravity loads according to EN 1990:2002 [35] and EN 1991-1-1:2002 [36], and wind-induced vibrations according to EN 1991-1-4:2005 Annex B [37] and ISO 10137:2007 [38]. The beams and columns were assumed to be spruce glued laminated timber with a strength class of GL24h. For the design of the cross-sections, strength and stiffness parameters were assumed from EN 14080:2013 [34]. The members and connections were designed with EN 1995-1-1:2004 [21].

The load combination for the gravity loads was chosen for office buildings in category B. The beams were designed with the following load combination:

$$p_{Ed} = \xi \gamma_G g_k + \gamma_Q q_k, \quad (6)$$

where  $\xi$  is 0.85,  $\gamma_G$  is 1.35,  $\gamma_Q$  is 1.50,  $g_k$  is 3.5 kN/m<sup>2</sup>, and  $q_k$  is 3.0 kN/m<sup>2</sup>. For the design of the columns, the design gravity load  $p_{Ed}$  in Equation (6) was multiplied with the reduction factor  $\alpha_n$  in EN 1991-1-1:2002 [36] for multi-storey buildings.

The connections were designed against the load combination in Equation (6) with laterally loaded steel dowels and a slotted-in steel plate. Based on the joint slip  $K_{ser}=\rho_m^{1.5}d/23$  in EN 1995-1-1:2004 [36], the connection stiffness  $k_\theta$  was computed with:

$$k_\theta = K_{ser} \sum_i^{n_d} r_i^2, \quad (7)$$

where index  $n_d$  is the number of dowels in the connection, and  $r_i$  is the distance of each dowel from the connection's centre of rotation. To find the connection stiffness per shear plane  $k_\theta$  in Equation (7), the spacing of the dowels was chosen as the minimum spacing in EN 1995-1-1:2004 [36]. The resulting connection stiffness  $k_\theta$  was 210 kNm/rad. The connections were assumed to be rigid on the column-side of the beam-column connection.

In the serviceability wind-design, terrain category III and a mean wind velocity of 26 m/s were chosen. Since the frames were symmetrical, only a planar frame was considered in the design against wind-induced vibrations. For the wind-design and the collapse simulations, a damping ratio  $\zeta$  of 2% was chosen based on ambient vibration tests [39].

In the collapse simulations, the following accidental load combination from EN 1990:2002 [35] was used:

$$p_{Ed} = g_k + \psi_{2,1} q_k, \quad (8)$$

where  $g_k$  is 3.5 kN/m<sup>2</sup>,  $q_k$  is 3.0 kN/m<sup>2</sup>, and  $\psi_{2,1}$  is 0.3. For all the frames, the initial damage scenario was the rapid loss of a ground-floor corner column.

### 3.2 FRAME CONFIGURATIONS

The frames were symmetrical in the horizontal plane with four bays and storeys. The beams and columns were placed on an orthogonal grid with a uniform spacing of 3600 mm in each axis direction. Two variations of the beam cross-sections were designed: (1) optimised for maximum utilisation; and (2) 50% utilisation. Both variations were designed for ultimate and serviceability limit states with EN 1995-1-1:2004 [21] with standard glued laminated timber dimensions. Bending stresses in the ultimate limit state was the governing design criterion for the design of the beams.

In the connection design, a dowel diameter of 8 mm and a steel plate thickness of 10 mm were chosen with an S235 steel quality. The dowels were arranged in a 3×2 rectangular pattern. With this layout, the shear capacity of the connection was 30 kN. The rotational stiffness of the connection  $k_{\theta}$  was 210 kNm/rad, which resulted in a peak acceleration of the softest frame of 0.053 m/s<sup>2</sup>. This satisfies the serviceability criterion of office buildings for wind-induced vibrations in ISO 10137:2013 [38]. For the collapse simulations, a linear-elastic behaviour of the connections and the members was assumed. The incremental damping scheme in Section 2.2.2 was adopted for the collapse simulations, with a damping ratio  $\zeta$  of 2%. An overview of the different frames is shown in Table 1.

**Table 1:** Beam and column cross-sections of the frames.

| No.      | Damage | Cross-section $b \times h$ (mm) |         |
|----------|--------|---------------------------------|---------|
|          |        | Beam                            | Column  |
| 120×240C | Corner |                                 |         |
| 120×240E | Edge   | 120×240                         | 360×360 |
| 120×240I | Inner  |                                 |         |
| 120×320C | Corner |                                 |         |
| 120×320E | Edge   | 120×320                         | 360×360 |
| 120×320I | Inner  |                                 |         |

## 4 RESULTS AND DISCUSSION

Both the models with the smaller and larger beam cross-sections suffered from near identical collapses when comparing the same column removal scenarios, as shown in Figure 2. This was because of the same failure modes being activated after column removal. In each simulation, after the column removal, the loads were diverted to the beams above the removed column, resulting in increased moments in the connections. The connections of the beams adjacent to and above the removed column were the first to exceed their capacity. For each damage-scenario, the damage propagated progressively from the removed column. The damage-scenario with the least collapsed floor area was the removal of the corner-column with a collapsed floor area of 6.3%, or 51 m<sup>2</sup>, including the roof. For the edge-column removal, the collapsed floor area was 12.5% or 104 m<sup>2</sup>, and 25% or 207 m<sup>2</sup> for the internal column removal.

The initial maximum static deformations of the frames before the column removals were 10.5 mm for the 120×240 scenarios and 5.6 mm for the 120×320 scenarios.

After the progressive collapses, the remaining members almost returned to their initial static deflections because of the complete vertical collapses of the bays adjacent to the removed columns. This is also because of the absence of inelastic material behaviour in the model.

Although the failure criterion of the connections was the maximum rotation  $\theta_y$ , the maximum deformations of the models at the first failure  $w_f$  were different. This can be attributed to the dynamic response of the frames and is shown in Table 2 and is reflected in the maximum moments at the first failure  $M_f$ . The progressive collapses of all the damage-scenarios stopped between a failure time  $t_f$  between 116 and 136 ms. The first failure in the corner column damage-scenario occurred up to 20 ms later than that of the internal damage-scenario. However, these differences are almost negligible and do not improve the robustness properties of the structure.

**Table 2:** Comparison of failure times  $t_f$ , durations of the collapse scenarios  $t_c$ , maximum deformations at the first failure  $w_f$ , and the corresponding moment  $M_f$  at the first failure.

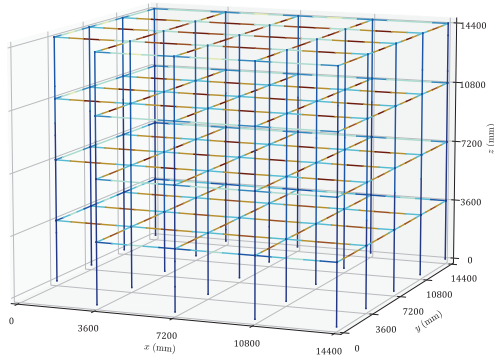
| No.      | $t_f$<br>(ms) | $t_c$<br>(ms) | $w_f$<br>(mm) | $M_f$<br>(kNm) |
|----------|---------------|---------------|---------------|----------------|
| 120×240C | 136           | 3             | 88.3          | 50.3           |
| 120×240E | 126           | 2             | 85.5          | 50.4           |
| 120×240I | 116           | 4             | 78.2          | 48.9           |
| 120×320C | 136           | 4             | 89.4          | 49.7           |
| 120×320E | 129           | 3             | 88.2          | 51.4           |
| 120×320I | 124           | 4             | 88.6          | 49.9           |

### 4.1 COLLAPSE MITIGATION

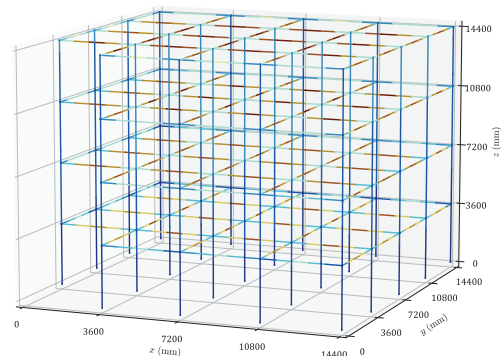
Here, suggestions are made for how the structure could be modified to increase its robustness and also how the model could capture other effects. Because the connections are the primary cause of the progressive collapses in the damage-scenarios, adjustments to their design could improve the robustness. However, changing one property of the connections could directly influence other properties. This can be exemplified in the following scenario. An increase of the moment capacity  $M_y$  may be conducted by increasing the distances of the fasteners in a laterally loaded timber connection with dowel-type fasteners. The moment capacity increases proportionally to the distance of the dowels to the centre of rotation of the connection, and the stiffness  $k_{\theta}$  increases quadratically, according to Equation (7). Consequently, the elastic rotational capacity  $\theta_y = M_y/k_{\theta}$  will decrease with increased distances. An increased moment capacity  $M_y$  of the connection could activate an alternative load path via bending. However, a reduced rotational capacity  $\theta_y$  would constrain the development of other alternative load paths, which require larger member rotations to be activated. An example is catenary action [40,41]. Moreover, overly strong connections may cause failures of the beams, which in practice is undesirable since timber has a predominantly brittle failure mode in bending [42,43]. Therefore, the modification of connection design without consideration of the impact of this on the larger structure may not necessarily increase the robustness of the structure.

The activation of alternative load paths may cause a progressive collapse [44], similar to the collapse of the Bad Reichenhall ice-arena [45]. Here, transferring loads from a damaged member to the adjacent structure may overload the structure. Considering this, a partial but more confined collapse may be preferable, similar to the collapse of the Siemens Arena [45]. For the considered damage-scenarios, the collapse propagated vertically and is shown in Figure 2. Fuse elements may prevent the horizontal propagation of a collapse, but not a vertical

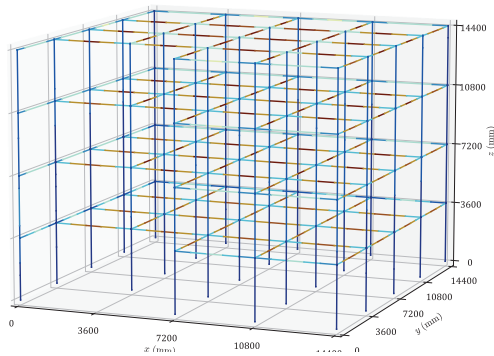
propagation [10]. To prevent the vertical propagation of a collapse, strong floors can be used for compartmentalization [10]. Future work could include scenarios where failure is not concentrated in the connections, and the effect of using members with a surplus capacity reserve could be evaluated. It is uncertain if this will be beneficial for the robustness of such structures, and if the increased material volume will justify such an approach.



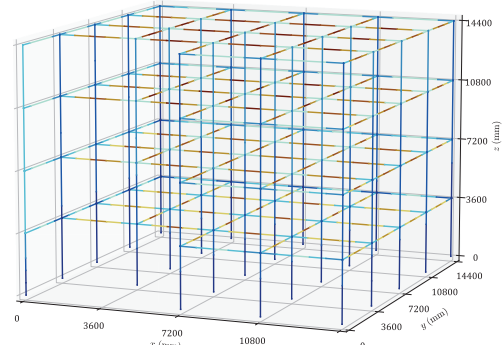
(a) 120x240C:  $t=139$  ms,  $w=10.53$  mm



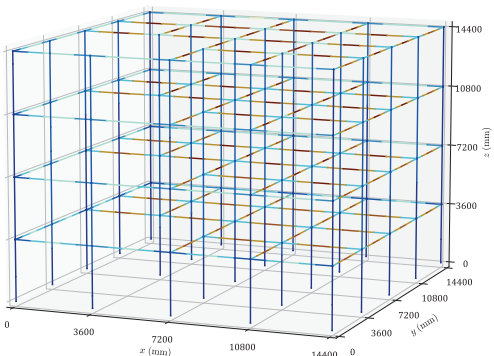
(b) 120x320C:  $t=140$  ms,  $w=5.58$  mm



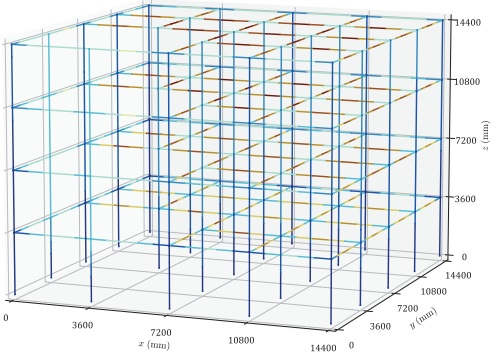
(c) 120x240E:  $t=128$  ms,  $w=10.53$  mm



(d) 120x320E:  $t=132$  ms,  $w=5.62$  mm



(e) 120x240I:  $t=120$  ms,  $w=10.54$  mm



(f) 120x320I:  $t=128$  ms,  $w=5.68$  mm

**Figure 2:** Maximum deformations for the frames with different beam cross-sections, immediately after the failure of the last element.

## 4.2 PLAUSIBILITY OF DEFORMATIONS

To evaluate the plausibility of the model, the two-dimensional static model depicted in Figure 3 was assessed for a corner-column damage-scenario. The structural system in Figure 3 is similar to the loading conditions in each storey above the removed column. To account for the stiffness of the laterally loaded timber connections with dowel-type fasteners, the beam ends were constrained by rotational springs with a rotational stiffness  $k_\theta$ , as defined in Section 3.2. The accuracy of the simplified beam model is more dependent on the rotational constraint than the axial constraint. For 120×240C, the maximum static deformation was 224 mm, and 213 mm for 120×320C.

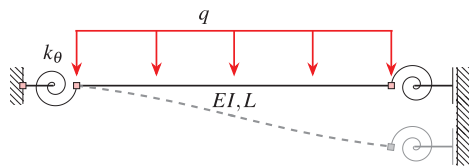


**Figure 3:** Simplified beam model of a corner-column damage-scenario.

To obtain comparable deformations to those of the simplified model, the nonlinear parametric collapse model was modified to neglect the failure of the connection elements. The maximum dynamic deformations from the column removal for 120×240C was 446 mm, and 425 mm for 120×320C. To compare the dynamic deformations from the nonlinear parametric collapse model and the static deformations from the simplified beam model, a dynamic amplification factor was necessary. Here, the dynamic amplification factor was defined as the ratio between the maximum dynamic and the maximum static deformations for the considered damage-scenario. For linear elastic structures without damping, the dynamic amplification factor attains a value of 2.0 [46]. Because of the limited damping for the considered structure, a dynamic amplification factor of 2.0 is reasonable [27]. With this dynamic amplification factor, the deviations between the parametric nonlinear collapse model and the simplified beam model are less than 0.25%. Therefore, the model results are reasonable.

## 4.3 LIMITATIONS

### 4.3.1 Connection behaviour

In the presented case study, the connection behaviour is linear elastic and perfectly brittle. This is a large simplification of the real behaviour of laterally loaded dowel-type connections with slotted-in steel plates, which could have hysteresis. The current iteration of the model neglects inelastic material behaviour, shear or tensile failure, as well as any energy dissipation from hysteretic behaviour. For connections which remain in the elastic domain, the modelled behaviour is realistic. For a column-removal scenario with no propagation of the failure, the linear-elastic connection assumption is conservative. This may not hold true if the collapse propagates further. Accounting for inelastic behaviour in the model would have increased the rotational capacity  $\theta_v$  and may increase the deformations of the members before failure. However,

including ductility in the inelastic behaviour of the connections may not increase the robustness of the structure [31]. For edge or internal column damage-scenarios, ductility in the connections could be beneficial. Here, the static system in Figure 3 remains a good approximation of the members above the removed column because of the symmetry. Ductility in the connections or member could cause larger deformations in the system and the activation of catenary action [40,41]. Further research should be conducted on the static and dynamic characterisation of the hysteretic behaviour of laterally loaded dowel-type connections with slotted in steel plates subjected to large deformations, combined loading, and full or partial load reversals.

### 4.3.2 Slabs and walls

Currently, the model offers a realistic depiction for frame-type buildings with non-load-bearing walls and disconnected floors. However, most buildings include floors and walls, which act as rigid diaphragms to transfer lateral loads. This behaviour is not reflected in the current model and may significantly influence the progressive collapse. Other researchers have shown that walls and slabs are beneficial for the structural robustness [41,47]. Hence, including walls and slabs in future models is important to expand the scope of the model.

### 4.3.3 Damping formulation

There are notable uncertainties related to the level of damping in the model, which are also difficult to quantify. The implemented amount of damping corresponds to a service-level situation in timber buildings. However, the level of damping in a progressive collapse of a timber building is not known. A collapse situation is also an extreme loading scenario with large deformations and nonlinearities [9], which is dissimilar to the situations in which previous measurements were conducted [39]. The amount of modelled damping may therefore be severely under- or overestimated. Moreover, there is not a clear consensus in the scientific community on how damping should be modelled in such situations [32].

Because glued laminated timber can be considered as a linear-elastic perfectly brittle material, it is safe to assume that any plasticity and energy dissipation will mainly be in the connections. Therefore, implementing hysteretic connection behaviour can reduce the uncertainties related to damping. By introducing damping directly into the connections, the incremental damping can be reduced to a minimum, which will also reduce the modelling uncertainties. Like the connection behaviour, the neglect of damping in a column-removal scenario with no propagation of the failure is conservative.

### 4.3.4 Model validation

The presented model is not validated with physical column-removal experiments. Because of the intrinsic nature of a collapse, it is difficult to conduct building-scale validation experiments. However, the individual modules of the model which require the input of physical parameters can be validated by component-scale experiments. The validation of the full model can be conducted with full-size dynamic member-removal

experiments on building sub-assemblies. Previously, the implemented mixed element method was verified against the finite element method for both static and dynamic analysis. Moreover, an extensive experimental campaign on impact loading of full-size timber beams was conducted to improve the modelling of the impact loading and the energy-based failure criterion.

## 5 CONCLUSIONS

In this paper, a nonlinear dynamic model was presented for investigating the progressive collapse of timber buildings. The model is fully parametric and can model the entirety of a progressive collapse, including features such as member failure, element removal, debris tracking, impact loading, and incremental damping. The model was demonstrated on symmetrical three-dimensional frames with four floors and bays. One frame was designed for a maximum utilisation in the ultimate limit state, and another for a 50% utilisation. The frames were subjected to a corner, edge, and internal column-removal scenario. All simulations resulted in vertically propagating collapses in the bays above the removed column. This was because of the failure of connections in bending. These connections acted as fuse elements and inhibited the horizontal propagation of damage. The capacity reserve in the beams was not activated because of the prior failure of the connections and did not lead to an increased robustness. Increasing the strength of the connections could activate alternative load paths via bending and an increase of the rotational capacity could do so through catenary action. However, a strength increase may not lead to an increase in the rotational capacity and further research is needed to assess the consequences on the failure mode of structures undergoing a column removal scenario.

The presented results are valid for frame-type structures with non-load-bearing walls and disconnected slabs. However, many structures have load slabs and walls acting as diaphragms. The current iteration of the collapse model cannot assess the contribution of these members. Similarly, trusses are also not implemented at the time of writing. These features are planned for the next iteration of the model. Besides the aforementioned limitations, the current incremental damping scheme is based on Rayleigh damping with fixed calibration factors with a damping ratio based on serviceability measurements of the damping ratio. There are several uncertainties related to the damping in this paper. To increase modelling accuracy and to reduce the uncertainties related to damping, more numerical and experimental research is needed.

The results in this paper were for linear elastic and perfectly brittle connections. However, the best practice in timber engineering is to design the connections with ductile behaviour. Future investigations should include inelastic connection behaviour to include connection hysteresis and the possible activation of alternative load paths.

The presented collapse model is an important step in the quantification and prevention of progressive and disproportionate collapse of timber buildings. The plausibility of the deformations in the model was verified

with a simplified beam model. However, there are still some hurdles left before the model can be used on a large scale. One of the main challenges is the validation of the model, which is only possible through full-size experiments of an entire building or a representative sub-assembly. Despite the aforementioned limitations, the presented model is an important step for assessing the robustness of timber structures.

## ACKNOWLEDGEMENT

This article is part of the project *Robustness of tall timber buildings* at ETH Zurich and is generously funded by the Albert Lück-Stiftung.

## REFERENCES

- [1] Starossek U, Haberland M. Disproportionate Collapse: Terminology and Procedures. *Journal of Performance of Constructed Facilities* 2010;24:519–28. [https://doi.org/10.1061/\(asce\)cf.1943-5509.0000138](https://doi.org/10.1061/(asce)cf.1943-5509.0000138).
- [2] Lalkovski N, Starossek U. The Total Collapse of the Twin Towers: What It Would Have Taken to Prevent It Once Collapse Was Initiated. *Journal of Structural Engineering* 2022;148. [https://doi.org/10.1061/\(asce\)st.1943-541x.0003244](https://doi.org/10.1061/(asce)st.1943-541x.0003244).
- [3] Adam JM, Parisi F, Sagaseta J, Lu X. Research and practice on progressive collapse and robustness of building structures in the 21st century. *Eng Struct* 2018;173:122–49. <https://doi.org/10.1016/j.engstruct.2018.06.082>.
- [4] Landolfo R, Formisano A, di Lorenzo G, di Filippo A. Classification of european building stock in technological and typological classes. *Journal of Building Engineering* 2022;45:103482. <https://doi.org/10.1016/j.job.2021.103482>.
- [5] Churkina G, Organschi A, Reyer CPO, Ruff A, Vinke K, Liu Z, et al. Buildings as a global carbon sink. *Nat Sustain* 2020;3:269–76. <https://doi.org/10.1038/s41893-019-0462-4>.
- [6] Ramage MH, Burr ridge H, Busse-Wicher M, Fereday G, Reynolds T, Shah DU, et al. The wood from the trees: The use of timber in construction. *Renewable and Sustainable Energy Reviews* 2017;68:333–59. <https://doi.org/10.1016/j.rser.2016.09.107>.
- [7] Crews KI. Nonconventional timber construction. *Nonconventional and Vernacular Construction Materials: Characterisation, Properties and Applications* 2020:437–66. <https://doi.org/10.1016/B978-0-08-102704-2.00016-0>.
- [8] Svatoš-Ražnjević H, Orozco L, Menges A. Advanced Timber Construction Industry: A Review of 350 Multi-Storey Timber Projects from 2000–2021. *Buildings* 2022;12:404. <https://doi.org/10.3390/buildings12040404>.
- [9] Huber JAJ, Ekevad M, Girhammar UA, Berg S. Structural robustness and timber buildings—a review. *Wood Mater Sci Eng* 2019;14:107–28. <https://doi.org/10.1080/17480272.2018.1446052>.
- [10] Mpodi Bitá H, Huber JAJ, Palma P, Tannert T. Prevention of Disproportionate Collapse for Multistory Mass Timber Buildings: Review of

- Current Practices and Recent Research. *Journal of Structural Engineering* 2022;148. [https://doi.org/10.1061/\(asce\)st.1943-541x.0003377](https://doi.org/10.1061/(asce)st.1943-541x.0003377).
- [11] Abed J, Rayburg S, Rodwell J, Neave M. A Review of the Performance and Benefits of Mass Timber as an Alternative to Concrete and Steel for Improving the Sustainability of Structures. *Sustainability (Switzerland)* 2022;14. <https://doi.org/10.3390/su14095570>.
- [12] Harte AM. Mass timber – the emergence of a modern construction material. *Journal of Structural Integrity and Maintenance* 2017;2:121–32. <https://doi.org/10.1080/24705314.2017.1354156>.
- [13] Cao AS, Stamatopoulos H. A theoretical study of the dynamic response of planar timber frames with semi-rigid moment-resisting connections subjected to wind loads. *Eng Struct* 2021;240. <https://doi.org/https://doi.org/10.1016/j.engstruct.2021.112367>.
- [14] Binck C, Cao AS, Frangi A. Lateral stiffening systems for tall timber buildings—tube-in-tube systems. *Wood Mater Sci Eng* 2022. <https://doi.org/10.1080/17480272.2022.2086066>.
- [15] Vilguts A, Stamatopoulos H, Malo KA. Parametric analyses and feasibility study of moment-resisting timber frames under service load. *Eng Struct* 2021;228:111583. <https://doi.org/10.1016/j.engstruct.2020.111583>.
- [16] Malo KA, Siem J, Ellingsbø P. Quantifying ductility in timber structures. *Eng Struct* 2011;33:2998–3006. <https://doi.org/10.1016/j.engstruct.2011.03.002>.
- [17] Buchanan AH. The challenges for designers of tall timber buildings. *WCTE 2016 - World Conference on Timber Engineering* 2016;25:24–35.
- [18] Franke S, Franke B, Harte AM. Failure modes and reinforcement techniques for timber beams-State of the art. *Constr Build Mater* 2015;97:2–13. <https://doi.org/10.1016/j.conbuildmat.2015.06.021>.
- [19] Ellingwood BR, Asce F. Mitigating Risk from Abnormal Loads and Progressive Collapse n.d. <https://doi.org/10.1061/ASCE0887-3828200620:4315>.
- [20] Cao AS, Frangi A. Mixed Element Method for Progressive Collapse Analysis: Method Description and Verification. In: di Trapani F, editor. *Proceedings of Eurasian OpenSees Days 2022*, Torino, Italy: Springer Nature; 2022.
- [21] European Committee for Standardization. EN 1995-1-1:2004. Eurocode 5: Design of timber structures - Part 1-1: General - Common rules and rules for buildings. Brussels, Belgium: 2004.
- [22] Cao AS, Houen MT, Lolli M, Frangi A. Pendulum Impact Hammer Tests on Glued Laminated Timber Beams. Zurich: 2022. <https://doi.org/10.3929/ethz-b-000585619>.
- [23] Cao AS, Lolli M, Frangi A. Pendulum impact hammer tests on spruce GLT – Preliminary results. In: Topping BHV, Kruis J, editors. *Proceedings of the Fourteenth International Conference on Computational Structures Technology*, Edinburgh, UK: Civil-Comp Press; 2022, p. 1–8.
- [24] Cao AS, Houen M, Lolli M, Frangi A. Pendulum impact hammer tests on glued laminated timber beams. Report 2022-01. Zurich, Switzerland: 2022. <https://doi.org/10.3929/ethz-b-000585619>.
- [25] Cao AS, Frangi A. Pendulum impact hammer tests on timber beams - Experimental setup. *WCTE 2023 - World Conference on Timber Engineering* 2023.
- [26] McKenna F, Scott MH, Fenves GL. Nonlinear Finite-Element Analysis Software Architecture Using Object Composition. *Journal of Computing in Civil Engineering* 2010;24:95–107. [https://doi.org/10.1061/\(asce\)cp.1943-5487.0000002](https://doi.org/10.1061/(asce)cp.1943-5487.0000002).
- [27] Cao AS, Palma P, Frangi A. Column removal analyses of timber structures - Framework to assess dynamic amplification factors for simplified structural design methods. *World Conference on Timber Engineering 2021, WCTE 2021*, Santiago, Chile: 2021, p. 1717–24.
- [28] Doudak G, Viau C, Lacroix D. Proposed design methodologies for timber assemblies subjected to blast loading. In: Görlacher R, editor. *International Network on Timber Engineering Research, INTER: Proceedings, Meeting 55, 21-25 August 2022*, Bad Aibling, Germany, Bad Aibling, USA: Timber Scientific Publishing, KIT Holzbau und Baukonstruktionen; 2022, p. 1–15.
- [29] U.S. Army Corps of Engineers, Naval Facilities Engineering Command, Air Force Civil Engineer Support Agency. UFC 4-023-03 Design of Buildings to Resist Progressive Collapse. 2009.
- [30] European Committee for Standardization. EN 1991-1-7:2006. Eurocode 1: Actions on structures - Part 1-7: General actions - Accidental actions. Brussels, Belgium: 2006.
- [31] Voulpiotis K, Schär S, Frangi A. Quantifying robustness in tall timber buildings: A case study. *Eng Struct* 2022;265:114427. <https://doi.org/10.1016/J.ENGSTRUCT.2022.114427>.
- [32] Chopra AK, McKenna F. Modeling viscous damping in nonlinear response history analysis of buildings for earthquake excitation. *Earthq Eng Struct Dyn* 2016;45:193–211. <https://doi.org/10.1002/eqe.2622>.
- [33] Schilling S, Palma P, Steiger R, Frangi A. Probabilistic description of the mechanical properties of glued laminated timber made from softwood. In: Görlacher R, editor. *International Network on Timber Engineering Research, INTER: Proceedings, Meeting 54, 16-19 August 2021*, Online, Timber Scientific Publishing, KIT Holzbau und Baukonstruktionen; 2021, p. 1–16.
- [34] European Committee for Standardization. EN 14080:2013 Timber structures - Glued laminated timber and glued solid timber - Requirements. Brussels, Belgium: 2013.
- [35] European Committee for Standardization. EN 1990:2002. Eurocode - Basis of structural design. Brussels, Belgium: 2002.
- [36] European Committee for Standardization. EN 1991-1-1:2002. Eurocode 1: Actions on structures - Part 1-1:2002. Eurocode 1: Actions on structures - Part 1-

- 1: General actions - Densities, self-weight, imposed loads for buildings. Brussels, Belgium: 2002.
- [37] European Committee for Standardization. EN 1991-1-4. Eurocode 1: Actions on structures -Part 1-4: General actions -Wind actions. Brussels, Belgium: 2005.
- [38] International Organization for Standardization. ISO 10137:2007. Bases for design of structures - Serviceability of buildings and walkways against vibrations. Geneva, Switzerland: 2007.
- [39] Feldmann A, Huang H, Chang W, Harris R, Gräfe M, Hein C. Dynamic properties of tall timber structures under wind-induced vibration. WCTE 2016 - World Conference on Timber Engineering, 2016.
- [40] Cao AS, Grönquist P, Frangi A. Manuscript under peer review: Catenary action in strip-reinforced wood and timber beams. *Constr Build Mater* 2023.
- [41] Mpidi Bitá H, Tannert T. Disproportionate collapse prevention analysis for post and beam mass timber building. *Journal of Building Engineering* 2022;56:104744.  
<https://doi.org/10.1016/J.JOBE.2022.104744>.
- [42] Ottenhaus L, Jockwer R, Drimmelen D Van, Crews K. Designing timber connections for ductility – A review and discussion. *Constr Build Mater* 2021;304:124621.  
<https://doi.org/10.1016/j.conbuildmat.2021.124621>.
- [43] Jorissen A, Fragiaco M. General notes on ductility in timber structures. *Eng Struct* 2011;33:2987–97.  
<https://doi.org/10.1016/J.ENGSTRUCT.2011.07.024>.
- [44] Voulpiotis K, Köhler J, Jockwer R, Frangi A. A holistic framework for designing for structural robustness in tall timber buildings. *Eng Struct* 2021;227:111432.  
<https://doi.org/10.1016/j.engstruct.2020.111432>.
- [45] Munch-Andersen J, Dietsch P. Robustness of large-span timber roof structures - Two examples. *Eng Struct* 2011;33:3113–7.  
<https://doi.org/10.1016/j.engstruct.2011.03.015>.
- [46] Li Y, Lu X, Guan H, Ye L. An energy-based assessment on dynamic amplification factor for linear static analysis in progressive collapse design of ductile rc frame structures. *Advances in Structural Engineering* 2014;17:1217–25.  
<https://doi.org/10.1260/1369-4332.17.8.1217>.
- [47] Huber JAJ, Mpidi Bitá H, Tannert T, Berg S. Finite element analysis of alternative load paths to prevent disproportionate collapse in platform-type CLT floor systems. *Eng Struct* 2021;240:112362.  
<https://doi.org/10.1016/j.engstruct.2021.112362>.